ECS Transactions, 77 (10) 149-156 (2017)
10.1149/07710.0149ecst ©The Electrochemical Society

Assessment of Sulfur Poisoning of Ni/CGO-Based SOFC Anodes

M. Riegraf[a], A. Zekri[b], V. Yurkiv[c], R. Costa[a], G. Schiller[a], K. A. Friedrich[a]

[a] German Aerospace Centre (DLR), Institute of Engineering Thermodynamics, 70569 Stuttgart, Germany
[b] University of Oldenburg, EHF Laboratory, Department of Physics, 26129 Oldenburg, Germany
[c] University of Illinois, Department of Mechanical and Industrial Engineering, Chicago, Illinois 60607, USA

The presence of fuel impurities, such as hydrogen sulfide, siloxane and phosphine, in biogas, diesel and natural gas can cause Solid Oxide Fuel Cell (SOFC) degradation due to surface poisoning of Ni-containing anodes. In this regard, Ni/CGO anodes have shown higher sulfur tolerance than Ni/YSZ anodes and a comparable high performance. In order to allow for a more profound understanding of the processes underlying sulfur poisoning, this study presents an extensive experimental investigation of commercial Ni/CGO-based SOFC operating on H_2/H_2O fuel gases and reformate fuel mixtures with trace amounts of hydrogen sulfide (H_2S). The short-term poisoning behavior of high-performance electrolyte-supported Ni/CGO10-based cells was systematically investigated by means of transient voltage stability experiments and electrochemical impedance measurements for a wide range of operating conditions. The effects of temperature (800 – 950 °C) and current density (OCV – 0.75 $A \cdot cm^{-2}$) on the extent of sulfur poisoning (1 – 20 ppm H_2S) was evaluated. The poisoning behavior was shown to be completely reversible for short exposure times in all cases. The chemical capacitance of Ni/CGO10 anodes was demonstrated to be strongly dependent upon temperature and gas phase composition reflecting a changing Ce^{3+}/Ce^{4+} ratio in the CGO phase. Using a model reformate as fuel gas, it was shown that CO can still be electrochemically converted under sulfur exposure. Furthermore, long-term experiments of 1500 h were conducted at 900 °C and 0.5 $A \cdot cm^{-2}$ with and without sulfur exposure and the degradation progress was monitored by impedance spectroscopy.

Introduction

Most prospective SOFC fuels such as biogas and natural gas contain undesirable sulfur-containing compounds that lead to the poisoning of the most common Ni/YSZ fuel electrodes causing a significant SOFC performance decrease (1–6). In this context, Ni/CGO based electrodes display a higher tolerance toward sulfur poisoning. Despite their high resistivity, to date only few studies have been dedicated to sulfur poisoning of Ni/CGO anodes (7–12).
While the performance decrease of SOFC with Ni/YSZ anodes was shown to be due to the poisoning of the Ni surface with elemental sulfur, recent fundamental studies of Ni/CGO anodes have indicated that the electrochemistry rather occurs on the CGO surface (double-phase boundary) than at the triple phase boundary (TPB) of Ni/CGO/gas phase. This suggests the Ni phase to be merely an electronic conductor (13–15). Since cerium in the CGO based

anodes possesses a mixed oxidation state at relevant operating conditions in reducing atmospheres, meaning that it can easily hop between Ce^{3+} and Ce^{4+}, it provides CGO its mixed ionic/electronic conductivity and high catalytic surface activity towards H_2 oxidation (7,9,13,14,16–20).

Several research groups have experimentally investigated the influence of sulfur-containing fuels on Ni/CGO-based SOFC performance (7–12). However, no reports of a systematic parameter study of sulfur poisoning or the long-term degradation effects on Ni/CGO were found in literature although this is vital in determining the acceptable limits of sulfur impurities in the fuels.

This work presents the experimental results of a detailed sulfur poisoning study of SOFC with Ni/CGO-based anodes. The short and long-term sulfur poisoning behavior of commercial, high-performance cells is examined at varying temperature and hydrogen sulfide concentration. The degradation behavior is monitored in-operando by means of electrochemical impedance spectroscopy.

Experimental Procedure

Two different kinds of commercial electrolyte-supported SOFC (hereafter named as cell A and cell B) were investigated that both employed a $Ni/Ce_{0.9}Gd_{0.1}O_{1.95}$(CGO10) anode. Cell A used a LSM/10Sc1CeSZ ($(Sc_2O_3)_{0.1}(CeO_2)_{0.01}(ZrO_2)_{0.89}$) composite cathode and a 10Sc1CeSZ electrolyte. Cell B employed a LSM/3YSZ cathode and a 3YSZ electrolyte. As the two cell types only differ in the electrolyte material, which is not present in the cermet anode, the behavior of the cells towards sulfur poisoning is considered to be the same. This was also confirmed beforehand by extensive characterization by means of electrochemical impedance spectroscopy (not shown here). The active area of the planar cells was 4 x 4 cm^2 with a total area of 5 x 5 cm^2. The setup for cell testing enables the characterization of up to four cells simultaneously and has been illustrated and described in detail elsewhere (12,21). All gases were supplied via mass flow controllers. H_2 was humidified in a water bubbler. H_2S was taken from a pressurized bottle containing 150 ppm H_2S in H_2. In order to avoid sulfur adsorption on the piping and its dissolution in the water bubbler, the sulfur was injected into the fuel stream after humidification right before the cell housing.

During short-time sulfur poisoning tests, the cells were operated with a H_2/H_2O fuel mixture in a ratio of 97:3 and different H_2S concentrations at a constant total fuel flow of 1 $L \cdot min^{-1}$ for each cell. The cathode was supplied with air at a constant flow of 2 $L \cdot min^{-1}$. The cells were heated (3 $K \cdot min^{-1}$) up to 950 °C for sealing and the NiO was subsequently reduced at 900 °C. The OCV was checked before starting the tests and confirmed to be higher than 1.2 V in pure hydrogen for all cells. For short-term sulfur poisoning measurements in H_2/H_2O fuels, sulfur poisoning experiments were conducted for cell A at 800 °C, 850 °C and 900 °C at a current density of 0.5 $A \cdot cm^{-2}$. For a systematic investigation of the sulfur poisoning behavior, the H_2S concentration was stepwise increased and set to 1, 2, 5, 10 and 20 ppm at each operating point.

For long-term degradation measurements, pure hydrogen was supplied and a current density of 0.5 $A \cdot cm^{-2}$ was set. A waiting time for cell voltage stabilization was observed. Sulfur poisoning experiments were subsequently started with cells of type B. Therefore, two cells were operated over 1500 h, one at a H_2S concentration of 1 ppm (with respect to the total gas flow rate) and one as a reference test without sulfur. In order to monitor the degradation

process, impedance measurements were carried out once a week (approximately 168 h). After the desired poisoning time was reached, the hydrogen sulfide supply was switched off, and the gas flow was substituted by pure H_2 to regenerate the anodes. Then, the cells were regenerated until the cell voltage stabilized again.

The cells were characterized by electrochemical impedance spectroscopy using an electrochemical workstation (Zahner® PP-240 with Thales software) in a frequency range between 50 mHz and 100 kHz with 8 points/decade. The amplitude of the current stimulus was chosen to be 500 mA and did not trigger a voltage response of higher than 15 mV.

Results and Discussion

The main objective of the present work is to assess the influence of sulfur poisoning on the performance and stability of Ni/CGO10 anodes. In order to obtain a detailed picture of the sulfur poisoning phenomena, firstly the short-term poisoning behavior and then the long-term poisoning behavior is presented.

Short-term poisoning of Ni/CGO anodes

The voltage stability tests over time are depicted for temperature variations between 800 °C and 900 °C in Figure 1 (left y-axis) together with the corresponding H_2S gas phase concentration (right y-axis). In all cases, the overall voltage drop increases stepwise with the H_2S concentration. The performance drop associated with the exposure of 1 ppm is the largest while the further increase of H_2S concentration only leads to smaller performance losses. For the exposure times investigated in the present study, full recovery was reached after switching off the sulfur supply at all operation points.

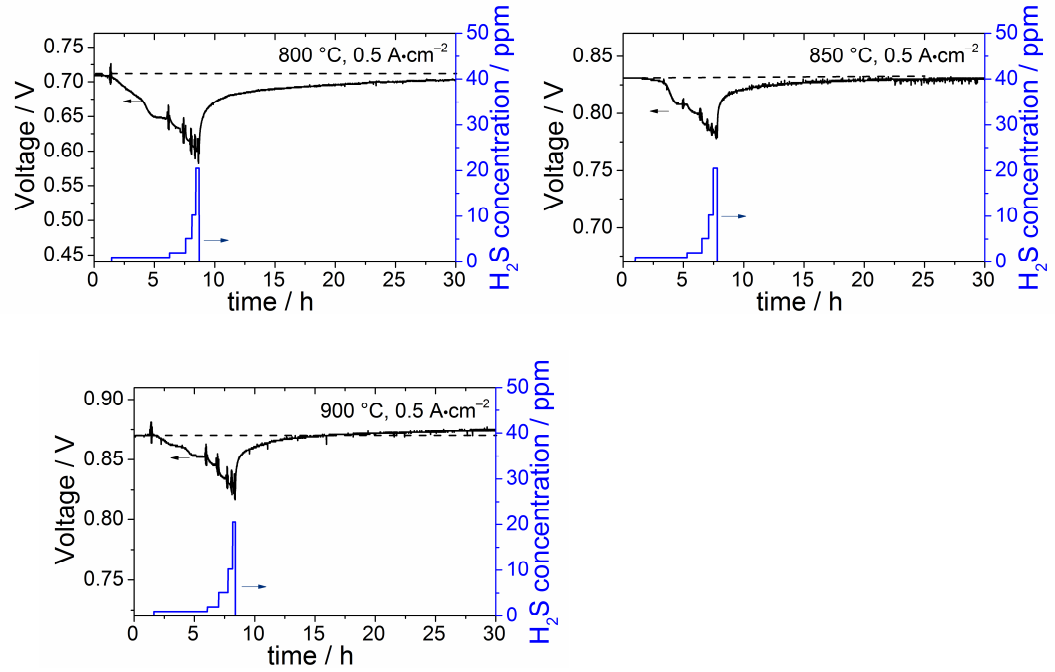

Figure 1. Short-term sulfur poisoning tests of cell A at $pO_2 = 0.21$ atm, $pH_2 = 0.97$ atm, $pH_2O = 0.03$ atm with an increasing H_2S concentration between 0 – 20 ppm (indicated on the right y-axis). The experiments were conducted at temperature (a) $T = 800$ °C (b) $T = 850$ °C (c) $T = 900$ °C and at a constant current density of $i = 0.5$ A•cm^{-2}.

The voltage drops for higher H_2S concentrations at 800 °C reach values of about 100 mV. These voltage drops already approach the magnitude of values observed for Ni/YSZ (22). This is a lot more severe in comparison to what earlier studies have reported for Ni/CGO anodes (7,23). So far, the reason for the significant performance drops in the present study is unclear. However, they suggest that the microstructure of Ni/CGO anodes possibly plays an important role in determining the sulfur tolerance.

Furthermore, the increasing voltage drops with temperature indicate a mitigating effect of temperature on the extent of sulfur poisoning. This is also confirmed by the increase of the area-specific resistance (ASR) in Figure 2, which is a more suitable measure for the sulfur poisoning than the cell voltage drop. A similar behavior has also already been observed for sulfur poisoning on Ni/YSZ anodes and was related to increasing desorption of H_2S from the Ni surface and consequently, a reduced sulfur surface coverage (24). This is a viable explanation as desorption processes are generally endothermic and hence, energetically more favorable with increasing temperature.

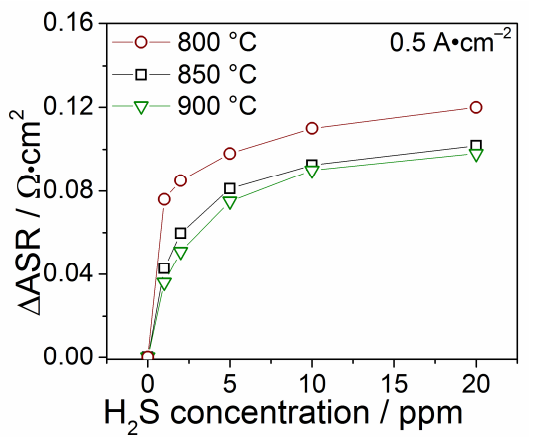

Figure 2. Accumulated ASR increase at a current density of 0.5 A·cm^{-2}, pO_2 = 0.21 atm, pH_2 = 0.97 atm, pH_2O = 0.03 atm, as a function of H_2S concentration at temperatures between 800 °C-900 °C.

Figure 3 shows differential imaginary impedance spectra of the recorded spectra at 1 ppm and 0 ppm for each temperature. Sulfur exposure mainly leads to an increase in the low-frequency region around about 0.1 Hz, which is consistent with the previous identification of an anode surface process at this frequency (11). This is approximately 4 orders of magnitude lower than the peak frequencies commonly observed for anode processes of Ni/YSZ-based SOFC (~10^3 – 10^4 Hz) that display an electric double layer capacitance at the interface between electrolyte (YSZ) and electrode (Ni) (1,5,25). Hence, it can be concluded that the capacitance of the observed Ni/CGO10 anode process is of a different nature than the one for Ni/YSZ suggesting fundamental differences in the hydrogen oxidation mechanisms. The low frequency of the observed anode surface process is in good agreement with the frequency of Ni/CGO10 electrode processes reported in literature (26,27).

The differential impedance spectra confirm the behavior observed in Figure 2 with a more pronounced increase of the intensity of the imaginary impedance at higher temperatures after exposing the anode to 1 ppm hydrogen sulfide. However, the peak frequency of the differential impedance spectra increases with decreasing temperature, indicating a change of the characteristic frequency of the low-frequency anode surface process as well. This is only

seldom observed for SOFC electrode processes, as thermally activated processes generally exhibit higher resistances at lower temperatures which results in a shift of the corresponding characteristic frequencies to lower values. Hence, the observed behavior must be caused by a significant decrease of capacitance with decreasing temperature.

It is well-known that double layer capacitances can be dependent on temperature (28), however, this influence is assumed to be negligible in many cases (29,30). The present results suggest that the chemical capacitance of the surface anode process leading to hydrogen oxidation on Ni/CGO10 is highly dependent on temperature. The chemical capacitance of this anode surface process is due to the mixed valent Ce^{3+}/Ce^{4+} and the Ce^{3+} bulk concentration has recently been shown to increase considerably with temperature, which is in good agreement with the capacitance changes observed in the present work (15,17,31).

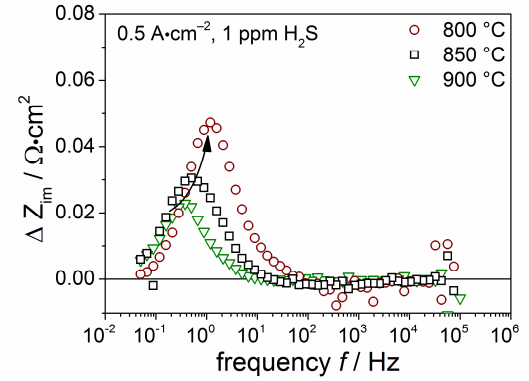

Figure 3. Differential imaginary impedance spectra for different temperatures at constant i = 0.5 A·cm^{-2}.

Long-term poisoning of Ni/CGO anodes

Figure 4 shows the cell voltage curves of the long-term poisoning measurements as a function of time for the two investigated cells at 0 and 1 ppm H_2S. Corresponding values for initial voltage, regenerated voltage and irreversible degradation are depicted in Table I.
For the 1 ppm-test, approximately the same voltage is recovered as the initial voltage drop. Surprisingly, during the course of the experiment of 1500 h, the irreversible degradation for the sulfur-exposed cell is only marginally larger (25 mV) than the one for the non-sulfur reference test (14 mV).

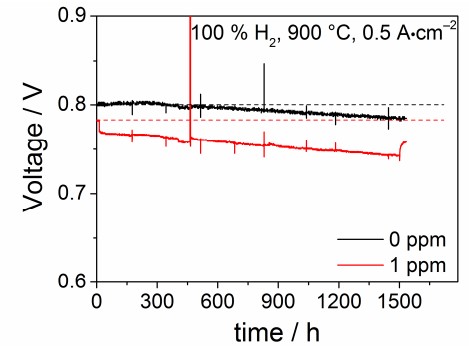

Figure 4. Cell voltage curves as a function of time at T = 900 °C and pO_2 = 0.21 atm. Cell of type B are operated at i = 0.5 A•cm^{-2}, pH_2 = 1.0 atm, and with H_2S concentrations of 0 and 1 ppm.

Performance changes during the test were also captured and can further be analyzed by the electrochemical impedance spectra in Figure 5. Upon sulfur exposure in the 1-ppm test, the impedance response in the frequency range 0.1-1 Hz rapidly increases, which is in agreement with the recently observed short-term poisoning behavior of these anodes. The non-sulfur reference test shows mainly an increase in the polarization resistance, specifically the higher frequency arc, which is associated with a cathode process (12). The resistance of this process also changes for the 1 ppm-test. For both tests, the low-frequency range that corresponds to the anode surface process remains unchanged over the poisoning period of the test, indicating no effect on the anode charge transfer process. However, in contrast to the 0 ppm-test, the 1 ppm-test shows an increase in ohmic resistance. The increase in polarization resistance of the cell is only small, suggesting the absence of considerable microstructural changes in the anode.

TABLE I. Overview of the cell voltage changes for the two long-term measurements. Initial and final voltage denote the cell voltages before the start of H_2S exposure, and after regeneration, respectively. The value for the initial voltage drop is calculated after 12 hours of sulfur exposure. The final voltage values were taken after 1500 h. The overpotential is calculated after the initial voltage drop.

Test acronym	Initial voltage [V]	Final voltage [V]	Irreversible degradation [mV]	Initial voltage drop [mV]	Regenerated voltage [mV]	Overpotential η [mV]
0 ppm	0.801	0.787	14	-	-	419
1 ppm	0.781	0.756	25	16	15	453

In a recent study of Ni/CGO40 anodes, Iwanschitz et al. have observed that the main contribution to the overall cell degradation after redox cycling was also an increase in ohmic resistance (19). This was in contrast to the same experiments on Ni/YSZ where redox cycling affected the high-frequency of the impedance spectra and Ni coarsening was observed. The authors witnessed that the electrical conductivity of the CGO40 drops after several redox cycles which could cause an increasing ohmic resistance as the CGO changes from a mixed ionic electronic conductor (MIEC) to a pure ionic conductor during the experiment. Recently it was shown that sulfur diffuses into the CGO phase after exposure (32,33). These studies demonstrate significant physicochemical interactions between sulfur and CGO, which suggests that the presence of high quantities of H_2S might lead to a drop in the electronic conductivity as observed for redox cycling.

On the whole, the demonstrated long-term stability of Ni/CGO anodes at 1 ppm H_2S is promising. However, in future experiments more harsh reaction conditions (higher hydrogen sulfide concentration, lower hydrogen partial pressure etc.) have to be chosen in order to fully assess the feasibility of Ni/CGO anode operation under sulfur exposure.

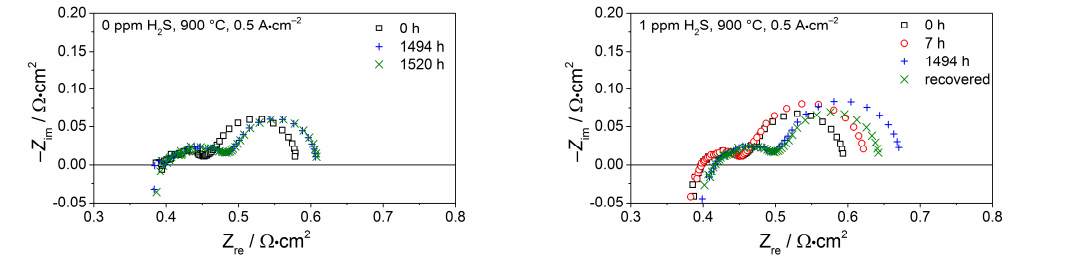

Figure 5. Nyquist plots of impedance spectra of the SOFC recorded at temperature T = 900 °C, and i = 0.5 A•cm^{-2}, pH$_2$ = 1.0 atm, and pO$_2$ = 0.21 atm, with different H$_2$S concentrations of (a) 0 ppm and (b) 1 ppm. Impedance spectra are shown at times t = 0 h (black squares), 7 h (red circles), 1494 h (blue plus sign) and 1520 h/after recovery (green cross).

Summary and Conclusions

In the present work an extensive experimental investigation of commercial Ni/CGO10-based SOFC operating on H$_2$/H$_2$O gas and reformate fuel mixtures with trace amounts of hydrogen sulfide (H$_2$S) was carried out. The short-term sulfur poisoning behavior of Ni/CGO10-based cells was systematically investigated by means of transient voltage stability experiments and electrochemical impedance measurements for a wide range of operating conditions varying H$_2$S concentration, temperature and current density. The poisoning behavior was shown to be completely reversible for short exposure times in all cases. The chemical capacitance of Ni/CGO10 anodes was demonstrated to be strongly dependent on temperature reflecting a changing Ce^{3+}/Ce^{4+} ratio in the CGO phase. Furthermore, long-term experiments of 1500 h were conducted at 900 °C and 0.5 A·cm^{-2} with 0 and 1 ppm H$_2$S. It could be shown that the introduction of 1 ppm H$_2$S only leads to a small increase of the degradation rate, which was accompanied by an increase of the ohmic resistance. The presented results give important insights into the degradation processes occurring during long-term operation of Ni/CGO anodes as well as strategies for stable SOFC operation. These promising low degradation rates demonstrate the feasibility of Ni/CGO anode operation under sulfur exposure and encourage further optimization of their performance and sulfur tolerance.

Acknowledgments

We gratefully acknowledge financial support by the German Ministry of Education and Research within the framework of the project “SOFC-Degradation: Analyse der Ursachen und Entwicklung von Gegenmaßnahmen” via grant number 03SF0494C. The authors are deeply grateful to Michael Hoerlein for help regarding test bench setup, cell testing and numerous scientific discussions.

References

1. M. Riegraf, G. Schiller, R. Costa, K. Andreas Friedrich, A. Latz, and V. Yurkiv, *J. Electrochem. Soc.*, **162**, F65 (2015).
2. A. Hagen, J. F. B. Rasmussen, and K. Thydén, *J. Power Sources*, **196**, 7271 (2011).
3. A. Hauch, A. Hagen, J. Hjelm, and T. Ramos, *J. Electrochem. Soc.*, **161**, F734 (2014).
4. A. Hagen, G. B. Johnson, and P. Hjalmarsson, *J. Power Sources*, **272**, 776 (2014).
5. A. Weber, S. Dierickx, A. Kromp, and E. Ivers-Tiffée, *Fuel Cells*, **13**, 487 (2013).

6. M. Riegraf, V. Yurkiv, G. Schiller, R. Costa, A. Latz, and K. A. Friedrich, *J. Electrochem. Soc.*, **162**, 1324 (2015).
7. S. Kavurucu Schubert, M. Kusnezoff, A. Michaelis, and S. I. Bredikhin, *J. Power Sources*, **217**, 364 (2012).
8. C. Xu, P. Gansor, J. W. Zondlo, K. Sabolsky, and E. M. Sabolsky, *J. Electrochem. Soc.*, **158**, B1405 (2011).
9. L. Zhang, S. P. Jiang, H. Q. He, X. Chen, J. Ma, and X. C. Song, *Int. J. Hydrogen Energy*, **35**, 12359 (2010).
10. E. Brightman, D. G. Ivey, D. J. L. Brett, and N. P. Brandon, *J. Power Sources*, **196**, 7182 (2011).
11. P. Lohsoontorn, D. J. L. Brett, and N. P. Brandon, *J. Power Sources*, **183**, 232 (2008).
12. M. Riegraf, V. Yurkiv, R. Costa, G. Schiller, and K. A. Friedrich, *ChemSusChem*, **10**, 587 (2017).
13. C. Zhang et al., *Nat. Mater.*, **9**, 944 (2010).
14. W. C. Chueh, Y. Hao, W. Jung, and S. M. Haile, *Nat. Mater.*, **11**, 155 (2011).
15. W. C. Chueh and S. M. Haile, *Phys. Chem. Chem. Phys.*, **11**, 8144 (2009).
16. Z. A. Feng, F. El Gabaly, X. Ye, Z.-X. Shen, and W. C. Chueh, *Nat. Commun.*, **5**, 1 (2014).
17. S. C. Decaluwe et al., *J. Phys. Chem. C*, **114**, 19853 (2010).
18. T. Nakamura, T. Kobayashi, K. Yashiro, A. Kaimai, T. Otake, K. Sato, J. Mizusaki, and T. Kawada, *J. Electrochem. Soc.*, **155**, B563 (2008).
19. B. Iwanschitz, J. Sfeir, A. Mai, and M. Schütze, *J. Electrochem. Soc.*, **157**, B269 (2010).
20. V. Papaefthimiou et al., *Adv. Energy Mater.*, **3**, 762 (2013).
21. M. P. Hoerlein, G. Schiller, F. Tietz, and K. A. Friedrich, *ECS Trans.*, **68**(1), 3553 (2015).
22. J. F. B. Rasmussen and A. Hagen, *J. Power Sources*, **191**, 534 (2009).
23. J. P. Ouweltjes, P. V. Aravind, N. Woudstra, and G. Rietveld, *J. Fuel Cell Sci. Technol.*, **3**, 495 (2006).
24. Y. Matsuzaki and I. Yasuda, *Solid State Ionics*, **132**, 261 (2000).
25. A. Hagen, *J. Electrochem. Soc.*, **160**, F111 (2013).
26. S. Primdahl and M. Mogensen, *Solid State Ionics*, **152**, 597 (2002).
27. A. Babaei, S. P. Jiang, and J. Li, *J. Electrochem. Soc.*, **156**, B1022 (2009).
28. M. G. H. M. Hendriks, J. E. Ten Elshof, H. J. M. Bouwmeester, and H. Verweij, *Solid State Ionics*, **146**, 211 (2002).
29. S. Gewies and W. G. Bessler, *J. Electrochem. Soc.*, **155**, B937 (2008).
30. M. Vogler, A. Bieberle-Hütter, L. Gauckler, J. Warnatz, W. G. Bessler, A. Bieberle-Hütter, L. Gauckler, J. Warnatz, and W. G. Bessler, *J. Electrochem. Soc.*, **156**, B663 (2009).
31. W. C. Chueh et al., *Chem. Mater.*, **24**, 1876 (2012).
32. M. Gerstl, A. Nenning, R. Iskandar, V. Rojek-Wöckner, M. Bram, H. Hutter, and A. Opitz, *Materials*, **9**, 649 (2016).
33. D. R. Mullins and T. S. McDonald, *Surf. Sci.*, **601**, 4931 (2007).